have decayed to $\Gamma \sim 10$ to 20 (*27*), corresponding to a relativistic beaming angle of ~3° to 6°. The measured upper limit on the polarization is therefore consistent with a small angle between the jet axis and our line of sight. While the probability of observing a jet at such a small viewing angle is small, there is independent evidence for beaming. The steepening of the light curve of the afterglow of GRB 990123, expected when Γ drops below $1/\theta$ (*7*, *28*) was observed about 2 days after the burst (*5*, *7*, *13, 29*). For $\Gamma \approx 5$ this corresponds to a jet opening angle of $\theta \sim 10°$. If the same beaming angle applies to the γ-rays (*30*) then the emitted energy in γ-rays alone is $E_\gamma \approx 8 \times 10^{52}$ erg (assuming a two-sided jet emission). The constraints on GRB formation scenarios are then considerably relaxed and possibly within reach of popular models based on stellar deaths.

References and Notes

1. T. Piran, *Phys. Rep.*, in press. Preprint available at http://xxx.lanl.gov/abs/astro-ph/9810256.
2. J. Heise *et al.*, in preparation.
3. C. W. Akerlof and T. A. McKay, *GCN Circular 205* (1999); *IAU Circular 7100* (1999); *Nature*, in press.
4. S. C. Odewahn, J. S. Bloom, S. R. Kulkarni, *GCN Circular 201* (1999); *IAU Circular 7094* (1999).
5. A. J. Castro-Tirado, *Science* **283**, 2069 (1999).
6. M. I. Andersen, *ibid.*, p. 2075.
7. S. R. Kulkarni *et al.*, *Nature*, in press. Preprint available at http://xxx.lanl.gov/abs/astro-ph/9902272.
8. A. S. Fruchter, *Astrophys. J.* **512**, L1 (1999).
9. J. F. C. Wardle and P. P. Kronberg, *Astrophys. J.* **194**, 249 (1974).
10. G. B. Taylor *et al.*, *Astrophys. J.* **502**, L115 (1998).
11. D. A. Frail, S. R. Kulkarni, J. S. Bloom, S. G. Djorgovski, *GCN Circular 141* (1998).
12. K. Serkowski, D. S. Mathewson, V. L. Ford, *Astrophys. J.* **196**, 261 (1975); A. Berdyugin and P. Teerikorpi, *Astron. Astrophys.* **318**, 37 (1997).
13. A. S. Fruchter *et al.*, preprint available at http://xxx.lanl.gov/abs/astro-ph/9902236.
14. J. S. Bloom *et al.*, in preparation. Preprint available at http://xxx.lanl.gov/abs/astro-ph/9902182.
15. S. Holland and J. Hjorth, *Astron. Astrophys.*, in press. Preprint available at http://xxx.lanl.gov/abs/astro-ph/9903175.
16. T. J. Galama *et al.*, *Nature*, in press. Preprint available at http://xxx.lanl.gov/abs/astro-ph/9903021.
17. S. G. Djorgovski, *et al.*, *GCN Circular 216* (1999).
18. C. C. Dyer and E. G. Shaver, *Astrophys. J.* **390**, L5 (1992); V. Faraoni, *Astron. Astrophys.* **272**, 385 (1993).
19. J. C. Brown and I. S. McLean, *Astron. Astrophys.* **57**, 141 (1977); S. R. Trammell, D. Hines, J. C. Wheeler, *Astrophys. J.* **414**, L21 (1993).
20. N. N. Chugai, *Sov. Astron. Lett.* **18**, 168 (1992).
21. P. Mèsz·ros and M. J. Rees, *Astrophys. J.* **476**, 232 (1997); R. Sari, T. Piran, R. Narayan, *ibid.* **497**, L17 (1998).
22. A. Gruzinov and E. Waxman, *ibid.* **511**, 852 (1999).
23. P. A. Hughes, H. D. Aller, M. F. Aller, *ibid.* **341**, 54 (1989); *ibid.*, p. 68; J. H. Fan, K. S. Cheng, L. Zhang, C. H. Liu, *Astron. Astrophys.* **327**, 947 (1997).
24. I. F. Mirabel and L. F. Rodriguez, *Ann. Rev. of Astron. Astrophys.*, in press. Preprint available at http://xxx.lanl.gov/abs/astro-ph/9902062.
25. A. Dar, *Astrophys. J.* **500**, L93 (1998); D. Fargion, preprint available at http://xxx.lanl.gov/abs/astro-ph/9808005.
26. A. Celotti and G. Matt, *Mon. Not. R. Astron. Soc.* **268**, 451 (1994).
27. R. Sari and T. Piran, preprint available at http://xxx.lanl.gov/abs/astro-ph/9902009 and http://xxx.lanl.gov/abs/astro-ph/9901338.
28. J. E. Rhoads, in preprint; P. Mesz·ros and M. J. Rees, preprint available at http://xxx.lanl.gov/abs/astro-ph/9902196.
29. I. A. Yadigaroglu and J. P. Halpern, *GCN Circular 248* (1999).
30. P. Mészáros, M. J. Rees, R. A. M. J. Wijers, preprint available at http://xxx.lanl.gov/abs/astro-ph/9808106.
31. Nilakshi, R. K. S. Yadav, V. Mohan, A. K. Pandey, R. Sagar, *Bull. Astron. Soc. India*, in press.
32. D. J. Schlegel, D. P. Finkbeiner, M. Davis, *Astrophys. J.* **500**, 525 (1998).
33. P. B. Stetson, *Publ. Astron. Soc. Pacific* **99**, 191 (1987); *ibid.*, p. 250 (1994).

34. We thank the NOT director and staff for their continued support to our GRB program. We are especially grateful to G. Cox for his swift action in mounting the calcite blocks at short notice. We have benefited from discussions with J. L. Gûmez and J. Knude. Insightful comments by R. A. M. J. Wijers and an anonymous referee improved the presentation of the results. This research was supported by the Danish Natural Science Research Council (SNF), the Icelandic Council of Science, and the University of Iceland Research Fund. The Nordic Optical Telescope is operated on the island of La Palma jointly by Denmark, Finland, Iceland, Norway, and Sweden in the Spanish Observatorio del Roque de los Muchachos of the Instituto de Astrofísica de Canarias. The data presented here have been taken using ALFOSC, which is owned by the Instituto de Astrofísica, Andalucía (IAA) and operated at the Nordic Optical Telescope under agreement between IAA and the Astronomical Observatory of the University of Copenhagen.

19 February 1999; accepted 5 March 1999

Spectroscopic Limits on the Distance and Energy Release of GRB 990123

Michael I. Andersen,[1]* Alberto J. Castro-Tirado,[2,3] Jens Hjorth,[4] Palle Møller,[5] Holger Pedersen,[4] Nicola Caon,[6] Luz Marina Cairós,[6] Heidi Korhonen,[1,7] María Rosa Zapatero Osorio,[6] Enrique Pérez,[3] Filippo Frontera[8]

An optical spectrum of the afterglow from the unusually bright gamma-ray burst GRB 990123 obtained on 24.25 January 1999 universal time showed an absorption system at a redshift of $z = 1.600$. The absence of a hydrogen Lyman α forest sets an upper limit of $z < 2.17$, while ultraviolet photometry indicates an upper limit of $z < 2.05$. The probability of intersecting an absorption system as strong as the one observed along a random line of sight out to this z is at most a few percent, implying that GRB 990123 was probably at $z = 1.600$. Currently favored cosmological parameters imply an isotropic energy release equivalent to the rest mass of 1.8 neutron stars (4.5×10^{54} erg) was emitted in gamma-rays. Nonisotropic emission, such as intrinsic beaming, may resolve this energy problem.

Intense bursts of gamma-rays, lasting from a fraction of a second to a couple of minutes, have been observed for three decades (*1*). During the past 2 years, ground-based follow-up observations have shown that almost all gamma-ray bursts (GRBs) with an optical afterglow have a cosmological origin (*2*). On 23 January at 9:47:14 universal time (UT), GRB 990123 was detected by the Italian-Dutch x-ray satellite BeppoSAX, several instruments on board the Compton Gamma Ray Observatory and other spacecraft. For BeppoSAX, this was the brightest GRB to date (*3*). The optical afterglow was identified shortly thereafter (*4, 5*). Optical emission with a magnitude of V = 8.95 at its maximum brightness was observed about 47 s after the start of the burst (GRB 990123 lasted about 100 s). The near coeval observations of a GRB and optical emission indicates that GRBs are associated with optical transients.

We obtained spectroscopic observations with the 2.56-m Nordic Optical Telescope (NOT), situated at Roque de Los Muchachos in La Palma, Canary Islands, on 24 January 1999 UT. The Andalucía faint object spectrograph and camera (ALFOSC) was used in long-slit mode with a 2048 × 2048 pixel charge-coupled device (CCD) detector, binned to a 1024 × 1024 pixel format to minimize detector noise. ALFOSC was configured with a 1.″2 wide slit and a 600 lines mm^{-1} grism blazed at 5600 Å. This gave a wavelength coverage from 3820 to 6830 Å with a dispersion of 3.0 Å per binned pixel

[1]Nordic Optical Telescope, Apartado 474 St. Cruz de La Palma, E-38700 Canarias, Spain. [2]Laboratorio de Astrofísica Espacial y Física Fundamental, Instituto Nacional de Técnica Aeroespacial, Post Office Box 50727, E-28080 Madrid, Spain. [3]Instituto de Astrofísica de Andalucía, Consejo Superior de Investigaciones Científicas, Post Office Box 03004, E-18080 Granada, Spain. [4]Astronomical Observatory, University of Copenhagen, Juliane Maries Vej 30, DK-2100 Copenhagen Ø, Denmark. [5]European Southern Observatory, Karl-Schwarzschild-Str. 2, D-85748 Garching bei München, Germany. [6]Instituto de Astrofísica de Canarias, E-38200, La Laguna, Tenerife, Spain. [7]Astronomy Division, University of Oulu, Post Office Box 3000, FIN-90401 Oulu, Finland. [8]Dipartimento di Fisica, Universitá di Ferara, Ferara, Italy.

*To whom correspondence should be addressed. E-mail: andersen@not.iac.es

and a spectral resolution of 9.5 Å. Three 40-min long-slit exposures were obtained between 4:49 and 6:54 UT, with zenith distances ranging from 45° to 26°. The position angle of the slit was about along the direction of the atmospheric dispersion, so a galaxy that was 10 arc sec west of GRB 990123 was also included in the slit. In between the individual exposures the telescope was offset by 2 arc sec along the direction of the slit. Immediately after the observations were acquired, the spectrophotometric standard star BD+332642 was observed and spectral lamp and flat fields were obtained. The flux-calibrated spectrum, resulting from combining the three individual spectra, is shown in Fig. 1. The wavelength calibration is precise to 0.5 Å root mean square (rms) with a maximum systematic shift of 1.5 Å.

Several absorption features are present in the spectrum. The identification of the lines is based on six ultraviolet Fe IIλλ1608, 2344, 2374, 2382, 2586, 2600 lines having identical redshifts and about the expected relative line ratios (the numbers give the rest wavelengths of the lines in angström). Identification of the remaining ultraviolet Si IIλλ1526, 1808, C IVλ1549, A1 IIλ1670, A1 IIIλλ1854, 1862, and Mg Iλ2026 lines follow from this (Table 1). The average z is 1.5999 with an rms scatter of 0.0004, omitting four lines which appear blended. The corresponding scatter in observed wavelength is 1.0 Å. The systematic error in the derived z is less than 0.0007 (*7*). A z of 1.5999 ± 0.0008 thus measured is consistent with that found from higher signal-to-noise spectrum obtained with the Keck-II telescope (*5*) 10 hours later. We note that the galaxy that is 10 arc sec west of GRB 990123 has a z of 0.278 ± 0.001.

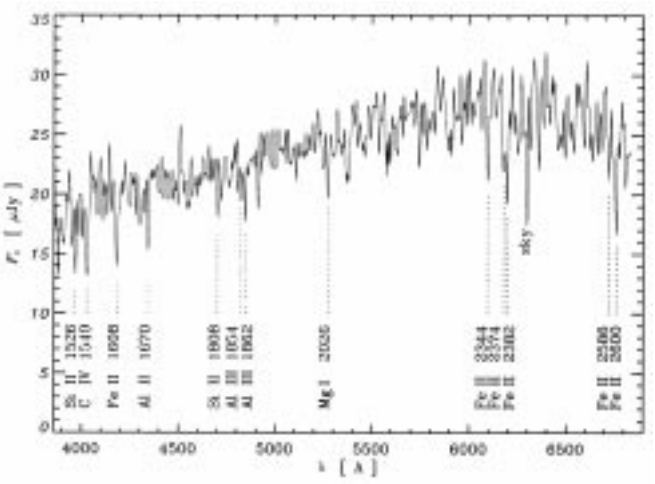

Fig. 1. The observed spectrum of the optical afterglow of GRB 990123 obtained at the Nordic Optical Telescope on 24.25 January 1999 UT, 19 hours after the burst. The identified with the absorber at $z = 1.5999$ are indicated (see also Table 1).

Table 1. Absorption features identified in the optical spectrum. The table gives the observed vacuum wavelength of the absorption features identified in the afterglow of the GRB 990123, the measured equivalent width for each line, its uncertainty and full width at half maximum (Å). The last four columns give the rest wavelength for the assigned physical absorption (Å), the inferred redshift, the difference between observed and expected wavelength (Å) for an average redshift of 1.5999 and the ionization state of the element, with an asterisk for lines that appear blended. In the Keck-II spectrum (*5*), two relatively strong spectral features are identified with the Zn IIλ 2026, 2062 and Cr IIλ 2062 lines. We are not able to confirm this, as the derived redshift following from this identification is inconsistent with the remaining lines (*7*).

λ_{obs}	W	±	FWHM	λ_{rest}	z	$\lambda_{obs} - \lambda_z$	ID
3969.0	2.3	1.1	7.0	1526.7	1.5997	−0.3	Si II
4027.5	4.3	0.9	13.1	1549.0	1.6001	0.3	C IV
4181.0	2.4	0.7	9.0	1608.5	1.5993	−0.9	Fe II
4343.9	2.4	0.5	8.4	1670.8	1.5999	0.0	Al II
4701.3	1.5	0.4	7.0	1808.0	1.6003	0.6	Si II
4823.5	1.1	0.4	8.3	1854.7	1.6007	1.5	Al III
4843.1	1.4	0.4	7.7	1862.8	1.5999	0.0	Al III
5270.9	1.7	0.4	11.1	2026.5	1.6008	2.0	Mg I*
6094.4	2.0	0.4	6.8	2344.2	1.5998	−0.3	Fe II
6176.5	2.6	0.4	7.9	2374.5	1.6012	3.0	Fe II*
6194.4	2.0	0.4	7.2	2382.8	1.5995	−0.6	Fe II*
6723.0	1.4	0.5	6.8	2586.7	1.5991	−2.2	Fe II*
6759.6	2.1	0.5	10.1	2600.2	1.5996	−0.7	Fe II

Table 2. Distances and energy output in various cosmologies. The first two columns give the cosmological density parameter Ω_0 and the contribution to the cosmic density from a cosmological constant Ω_Λ. The third column gives the luminosity distance to GRB 990123 at a redshift of 1.600 and the fourth column gives the corresponding distance modulus. The last two columns give the implied isotropic energy release in gamma-rays in erg or in units of the equivalent rest mass of a neutron star (assumed to have a mass of 1.4 solar masses). The Hubble constant is defined as $H_0 = 100\ h$ km s^{-1} Mpc^{-1}.

Ω_0	Ω_Λ	D_L ($10^{28}\ h^{-1}$ cm)	$m - M + 5 \log h$	$E\gamma$ ($10^{54}\ h^{-2}$ erg)	E_γ (1.4 h^{-2} $M_\odot$)
0.2	0.0	2.40	44.46	1.42	0.57
0.2	0.8	2.79	44.78	1.91	0.76
1.0	0.0	1.83	43.86	0.82	0.33

In the absence of intrinsic spectral features in the optical afterglow a definite distance to a GRB cannot be determined. The presence of the $z = 1.600$ absorption system gives a lower limit to the distance to GRB 990123. An upper limit can be determined by exploiting the fact that hydrogen clouds along any line of sight will give rise to strong absorption in the spectrum at wavelengths blue-wards of hydrogen Lyman-α (Lyα) at a rest wavelength of λ = 1216 Å (*2*), leading to a "Lyman α forest." For redshifts near and above 1.6 where the Lyman α forest is located in the observed ultraviolet. Our spectrum covers the region down to 3820 Å. The absence of a Lyman α forest above 3850 Å leads to an upper limit of $z < 2.17$ of GRB 990123.

The spectrum is described by a power law, $F_\nu \propto \nu^\beta$ for wavelengths shorter than 5700 Å, with $\beta = -0.69 \pm 0.10$. Our ultraviolet (U band) photometry (*8*) indicates that the U-band flux, when corrected to the mid-epoch of our observations by the power-law decay (*8*), is slightly above the extrapolated power law, but within the uncertainties of the power-law fit. The presence of a Lyman α forest in the U band data would imply a line blanketing from 6% (3300 Å) to 12% (3900 Å) (*9*). Taking into account the instrumental sensitivity function, if a Lyman α forest is present from 3700 Å, the average line blanketing in the U-band will be 0.06 magnitude corresponding to a 2-sigma error in the photometry (*8*). It is therefore possible that $z < 2.05$ for GRB 990123. We note, however, that this limit is based on an extrapolated spectrum of the afterglow and is sensitive to possible systematic errors in the photometric calibration of the U band data.

The identified absorption lines show a small scatter in the derived rest wavelength, which is accounted for by the photon noise in the spectrum. There is no indication of systematic differences in the derived redshifts of the different elements or ionization states. As the seeing was

about 1.″2, the true spectral resolution is around 8 Å, consistent with the measured width of the spectral features. The average line profile, constructed from the Fe II lines above 6000 Å, appears unresolved. This implies that the absorbing clouds have a velocity dispersion of less than 100 km s^{-1} in the rest frame.

The observed BATSE gamma-ray fluence of GRB 990123 is $5.09 \pm 0.02 \times 10^{-4}$ erg cm^{-2} for energies above 20 keV (*14*). In Table 2 we give the luminosity distance and the inferred isotropic energy output in various cosmologies for $z = 1.600$. A lower limit to the isotropic energy release in gamma-rays alone is obtained in an Einstein-de Sitter Universe with $(\Omega_0\Omega_\Lambda) = (1,0)$. For a upper limit to the Hubble constant of $H_0 < 80$ km s^{-1} Mpc^{-1} we find a lower limit of 0.5 times the rest mass of a neutron star (1.4 $M_\odot$-2.5×10^{54} erg) or ~2.5 times its binding energy. For a set of currently observationally-favored cosmological parameters $(\Omega_0\Omega_\Lambda)=(0.2, 0.8)$ and $H_0 = 65$ km s^{-1} Mpc^{-1} we derive an energy release in gamma-rays equivalent to 1.8 neutron stars. This is 45 times larger than the total energy emitted in all wavelengths by the most luminous Type II supernova, including neutrino emission (*15*).

If the GRB 990123 is located at $z > 1.6$ our upper limit on z translates into an upper limit on the energy release of 1.3×10^{55} erg for $H_0 > 50$ km s^{-1} Mpc^{-1} and $(\Omega_0\Omega_\Lambda) = (0.2, 0.8)$. Moreover, if the $z = 1.6$ absorption system is associated with the main mass component along the line of sight to GRB 990123, the upper limit on z leads to a required lensing surface mass density of a factor of about three to four times that in normal galaxy lenses. This effectively rules out the possibility that GRB 990123 was lensed (multiply imaged) (*16*) by this mass.

Any of the above numbers indicates a huge isotropic energy release which is difficult to reconcile with current physical theories. In the absence of lensing one resolution of this energy problem is that the gamma-ray emission from GRB 990123 was not isotropic. This interpretation is consistent with polarimetric observations (*17*) and is supported by the breaks observed in the light curve (*5, 8, 12*) which suggest that the optical afterglow may have been beamed.

References and Notes

1. G. J. Fishman and C. A. Meegan, *Annu. Rev. Astron. Astrophys.* **33**, 415 (1995).
2. M. R. Metzger *et al.*, *Nature* **387**, 879 (1997); S. R. Kulkarni *et al.*, *ibid.* **393**, 35 (1998); S. G. Djorgovski *et al.*, *Astrophys, J.* **507**, L25 (1998).
3. J. Heise, in preparation.
4. S. C. Odewahn, J. S. Bloom, S. R. Kulkarni, *GCN Circular 201* (1999); *IAU Circular 7094* (1999).
5. S. R. Kulkarni *et al.*, *Nature*, in press, preprint also available at http://www.lanl.gov/abs/astro-ph/9902272.
6. C. W. Akerlof and T. A. McKay, *GCN Circular 205* (1999); *IAU Circular 7100* (1999); *Nature*, submitted (1999).
7. A more comprehensive analysis of the absorption system will be presented in a paper in preparation.
8. A. J. Castro-Tirado *et al.*, *Science* **28X**, XXX (1999).
9. P. Møller and P. Jakobsen, *Astron. Astrophys.* **228**, 299 (1990).
10. M. Pettini, D. L. King, L. J. Smith, R. W. Hunstead, *Astrophys. J.* **478**, 536 (1997); M. Pettini, L. J. Smith, D. L. King, R. W. Hunstead, *ibid.* **486**, 665 (1997).
11. J. S. Bloom *et al.*, in preparation; preprint available at http://www.lanl.gov/abs/astro-ph/9902182.
12. A. S. Fruchter *et al.*, in preparation; preprint available at http://www.lanl.gov/abs/astro-ph/9902236.
13. S. Holland and J. Hjorth, *Astron. Astrophys.*, in press, preprint also available at http://www.lanl.gov/abs/astro-ph/9903175.
14. R. M. Kippen, *GCN Circular 224* (1999).
15. See *Thermonuclear Supernovae*, P. Ruiz-Lapuente, R. Canal, J. Isern, Eds. (Kluwer Academic, Dordrecht, Netherlands, 1997).
16. S. G. Djorgovski *et al.*, *GCN Circular 216* (1999).
17. J. Hjorth *et al.*, *Science* **28X**, XXX (1999).

18. We thank the NOT director for continued support to our GRB programme. This research was supported by the Danish Natural Science Research Council (SNF), the Icelandic Council of Science and the University of Iceland Research Fund. The Nordic Optical Telescope is operated on the island of La Palma jointly by Denmark, Finland, Iceland, Norway, and Sweden in the Spanish Observatorio del Roque de los Muchachos of the Instituto de Astrofísica de Canarias. The data presented here have been taken using ALFOSC, which is owned by the Instituto de Astrofísica de Andalucía (IAA) and operated at the Nordic Optical Telescope under agreement between IAA and the Astronomical Observatory of the University of Copenhagen.

23 February 1999; accepted 9 March 1999

A Simple Predictive Model for the Structure of the Oceanic Pycnocline

Anand Gnanadesikan

A simple theory for the large-scale oceanic circulation is developed, relating pycnocline depth, Northern Hemisphere sinking, and low-latitude upwelling to pycnocline diffusivity and Southern Ocean winds and eddies. The results show that Southern Ocean processes help maintain the global ocean structure and that pycnocline diffusion controls low-latitude upwelling.

The main oceanic pycnocline delineates the boundary between light, low-latitude surface waters and dense, abyssal waters whose properties are set in the high latitudes (Fig. 1A). The physical properties at work in the pycnocline and the flows driven by the pressure gradients associated with the pycnocline affect the transport of heat, salt, and nutrients through the ocean. Here I examine the relative importance of several key processes in setting the structure of the pycnocline. These are (i) vertical diffusion within the pycnocline, (ii) upwelling through the pycnocline in low latitudes, (iii) the conversion of light to dense water associated with the formation of North Atlantic Deep Water, (iv) Southern Ocean winds, and (v) Southern Ocean eddies. Previous scaling theories of the pycnocline (*1*) have only included the first three processes.

The western Atlantic Ocean contains a bowl of waters lighter than 1027.5 kg m^{-3} ~1000 m deep, with some upward deflection at the equator (*2*). A tongue of fresh Antarctic Intermediate Water (AAIW) penetrates northward from the Southern Ocean and a tongue of salty North Atlantic Deep Water (NADW) moves southward. In the conceptual framework I propose (Fig. 1C), surface cooling in the Northern Hemisphere (NH) leads to the conversion of light water to dense water, which flows southward at a rate T_n. Some portion of this flux upwells within the Southern Ocean, where precipitation causes it to become lighter. This light water is then exported to the north at a rate T_s. That portion of the NH sinking flux that is not balanced by upwelling within the Southern Ocean upwells through the low-latitude pycnocline at a rate T_u. I have ignored deep flows associated with the Antarctic Bottom Water (AABW), assuming that they have little direct effect on the pycnocline as they are returned at mid-depth (*3*). Instead I focus on the effect of Northern and Southern Hemisphere mode waters on the lower pycnocline.

These fluxes can be connected to the depth of the pycnocline, reducing the equations governing the large-scale oceanic circulation to a single cubic equation in the pycnocline depth D. The first step is to derive an expression for T_n, the NH sinking flux. It is common to assume that this flow is proportional to the density difference between the light and dense water $\Delta\rho$ (*4*). Because northward flow of AAIW and the southward flow of NADW are essentially pressure-driven, there is a level of no motion between the two flows at which the velocities and hence the pressure gradients are negligible. The mass of water above the level of no motion is thus the same at all latitudes. Because the warm waters in low latitudes are less dense, they take up more volume and the surface height is higher at the equator than in high latitudes. This surface height difference will cause a pressure differ-

National Oceanic and Atmospheric Administration (NOAA) Geophysical Fluid Dynamics Laboratory and Atmospheric and Oceanic Sciences Program, Princeton University, Post Office Box CN710, Princeton, NJ 08544, USA. E-mail: gnana@splash.princeton.edu